HHS Public Access

Author manuscript

Nature. Author manuscript; available in PMC 2012 May 10.

Published in final edited form as:

Nature. ; 479(7372): 237–240. doi:10.1038/nature10508.

ATM controls meiotic double-strand break formation

Julian Lange[1], **Jing Pan**[1,†], **Francesca Cole**[2], **Michael P. Thelen**[4], **Maria Jasin**[2], and **Scott Keeney**[1,3]

[1]Molecular Biology Program, Memorial Sloan-Kettering Cancer Center, 1275 York Avenue, New York, New York 10065, USA.

[2]Developmental Biology Program, Memorial Sloan-Kettering Cancer Center, 1275 York Avenue, New York, New York 10065, USA.

[3]Howard Hughes Medical Institute, Memorial Sloan-Kettering Cancer Center, 1275 York Avenue, New York, New York 10065, USA.

[4]Physical and Life Sciences Directorate, Lawrence Livermore National Laboratory, Livermore, California 94550, USA.

Abstract

In many organisms, developmentally programmed double-strand breaks (DSBs) formed by the SPO11 transesterase initiate meiotic recombination, which promotes pairing and segregation of homologous chromosomes[1]. Because every chromosome must receive a minimum number of DSBs, attention has focused on factors that support DSB formation[2]. However, improperly repaired DSBs can cause meiotic arrest or mutation[3,4], thus having too many DSBs is likely as deleterious as having too few. Only a small fraction of SPO11 protein ever makes a DSB in yeast or mouse[5], and SPO11 and its accessory factors remain abundant long after most DSB formation ceases[1], implying the existence of mechanisms that restrain SPO11 activity to limit DSB numbers. Here we report that the number of meiotic DSBs in mouse is controlled by ATM, a kinase activated by DNA damage to trigger checkpoint signaling and promote DSB repair. Levels of SPO11-oligonucleotide complexes, by-products of meiotic DSB formation, are elevated at least ten-fold in spermatocytes lacking ATM. Moreover, *Atm* mutation renders SPO11-oligonucleotide levels sensitive to genetic manipulations that modulate SPO11 protein levels. We propose that ATM restrains SPO11 via a negative feedback loop in which kinase activation by DSBs suppresses further DSB formation. Our findings explain previously puzzling phenotypes of *Atm*-null mice and provide a molecular basis for the gonadal dysgenesis observed in ataxia telangiectasia, the human syndrome caused by ATM deficiency.

Correspondence and requests for materials should be addressed to S.K. (s-keeney@ski.mskcc.org) or M.J. (m-jasin@ski.mskcc.org).
†Present address: Cell Biology Department, University of Texas Southwestern Medical Center, Dallas, Texas 75390, USA.

Supplementary Information is linked to the online version of the paper at www.nature.com/nature.

Author Contributions J.L., J.P., and F.C. performed experiments. M.P.T. generated the anti-SPO11 monoclonal hybridoma line. J.L., M.J., and S.K. wrote the paper.

Author Information The authors declare no competing financial interests. Reprints and permissions information is available at www.nature.com/reprints.

SPO11 creates DSBs via a covalent protein-DNA intermediate that is endonucleolytically cleaved to release SPO11 attached to a short oligonucleotide (oligo), freeing DSB ends for further processing and recombination[5] (Fig. 1a). SPO11-oligo complexes are a quantitative by-product of DSB formation that can be exploited to study DSB number and distribution[5–7] (Supplementary Fig. 1). We examined SPO11-oligo complexes by SPO11 immunoprecipitation and 3′-end-labeling of whole-testis extracts from *Atm*$^{-/-}$ mutant mice, which display multiple catastrophic meiotic defects, including chromosome synapsis failure and apoptosis[8–12]. The *Atm*$^{-/-}$ phenotype resembles that of mutants lacking DSB repair factors such as DMC1, indicating that absence of ATM causes meiotic recombination defects. While *Spo11*$^{-/-}$ mutation is epistatic to *Atm*$^{-/-}$ (refs 11,12), the functional relationship between ATM and SPO11 is complex, as meiotic defects of *Atm*$^{-/-}$ mice are substantially rescued by reducing *Spo11* gene dosage[13,14] (discussed below).

Unexpectedly, we found that adult *Atm*$^{-/-}$ testes exhibited an ~ten-fold elevation in steady-state levels of SPO11-oligo complexes relative to wild-type littermates (Fig. 1b) (11.3 ± 4.5-fold, mean and s.d., n=7 littermate pairs). This finding contrasts with *Dmc1*$^{-/-}$ testes, which displayed a ~50% reduction in SPO11-oligo complexes (0.51 ± 0.06-fold relative to wild type, n=5) (Fig. 1c), as previously shown[5,7]. The mutants share similar arrest points in prophase I, as determined by molecular and histological data[12], thus increased SPO11-oligo complexes in *Atm*$^{-/-}$ spermatocytes are not an indirect consequence of arrest or of an increased fraction of meiocytes harboring such complexes.

In *Atm*$^{-/-}$ testes, levels of free SPO11 (i.e., not bound to an oligo) were much lower than in wild type (Fig. 1b). This is not because a large fraction of SPO11 has been consumed in covalent complexes with DNA, which alters its electrophoretic mobility, as free SPO11 was not restored to wild-type levels by nuclease treatment (Fig. 1d). Instead, since *Spo11* transcript levels in wild type are highest in later stages of meiotic prophase[15–18], after the arrest point of *Atm*$^{-/-}$ cells, reduced free SPO11 is attributable to the lack of later meiotic cell types, consistent with the reduced free SPO11 also found in *Dmc1*$^{-/-}$ cells (Fig. 1c). As expected, the residual SPO11 protein in *Atm*$^{-/-}$, like *Dmc1*$^{-/-}$, testes was mostly SPO11β (Fig. 1b,c). SPO11α and SPO11β are major protein isoforms encoded by developmentally regulated splice variants; SPO11β is expressed earlier and is sufficient for nearly normal DSB levels[5,15,17–20].

Elevated SPO11-oligo complexes can be explained by an increased number of meiotic DSBs and/or a longer lifespan of complexes. To distinguish between these possibilities, we examined the initial appearance and persistence of SPO11-oligo complexes in juvenile mice, in which the first suite of spermatogenic cells proceeds through meiosis in a semi-synchronous fashion[21]. First, we assayed SPO11-oligo complexes in whole-testis extracts from wild-type C57BL/6J mice at post-natal days 7 to 24 (Fig. 2a). SPO11-oligo complexes first appeared between d9 and d10, when most cells of the initial cohort have entered leptonema. SPO11-oligo complexes persisted or increased slightly through d15, when the first cohort has progressed into pachynema. Levels rose still further from d16–d18, coincident with the second cohort of spermatogenic cells reaching leptonema[21]. Thus, SPO11-oligo complexes appear at the same time as cell types that experience the majority of meiotic DSBs. Consistent with findings in mutants (see above), only trace amounts of free

SPO11 protein were seen when SPO11-oligo complexes first appeared, with SPO11β the predominant isoform at these times (Fig. 2a). Importantly, SPO11-oligo complex levels did not decline between the first and second spermatogenic cohorts. We infer that the lifespan of the complexes is long relative to the duration of prophase, and that an increased lifespan is not a likely explanation for the large increase in steady-state SPO11-oligos in adult *Atm*$^{-/-}$ testes.

In support of this interpretation, we found that SPO11-oligo complexes were undetectable in *Atm*$^{-/-}$ testes at d7 (data not shown) but were already elevated 3.3-fold compared with a wild-type littermate when they first appeared, increasing to 8.4-fold over wild type by d12 (Fig. 2b). Since *Atm*$^{-/-}$ juveniles displayed higher SPO11-oligo levels as soon as the first leptotene cells appeared, we conclude that most, if not all, of the increase reflects a greater number of meiotic DSBs occurring during prophase I.

Meiotic defects of mice lacking ATM are substantially suppressed by reducing *Spo11* gene dosage: *Spo11*$^{+/-}$ *Atm*$^{-/-}$ spermatocytes pair and recombine their autosomes and progress through meiotic prophase to metaphase I, where they arrest due to a failure in sex chromosome pairing and recombination[13,14]. The reason for this puzzling rescue was unknown, but our current findings suggest an explanation: the majority of meiotic defects in *Atm*-null spermatocytes are caused by grossly elevated DSB levels, which are lowered by *Spo11* heterozygosity (which reduces SPO11 protein levels by half in adult and juvenile testes (ref. 17 and our unpublished data). Indeed, we found SPO11-oligo complexes in *Spo11*$^{+/-}$ *Atm*$^{-/-}$ mice to be substantially reduced compared with *Atm*$^{-/-}$ littermates (Fig. 3a). The remaining increase in SPO11-oligo complexes in *Spo11*$^{+/-}$ *Atm*$^{-/-}$ mutants compared with wild type (range of 4.5- to 7.8-fold, n=2) is not simply a consequence of metaphase arrest, because SPO11-oligo complexes were not elevated in mice that exhibit a similar arrest point due to absence of MLH1, a protein involved late in recombination[22] (Fig. 3a). The fact that DSBs are still elevated in *Spo11*$^{+/-}$ *Atm*$^{-/-}$ spermatocytes relative to wild type may account for some or all of the remaining defects in this mutant, including axis interruptions at sites of ongoing recombination and persistent unrepaired DSBs late in prophase I (ref. 14).

Our findings indicate that the absence of ATM renders the extent of DSB formation sensitive to SPO11 expression levels. Therefore, we reasoned that increasing SPO11 expression should further elevate DSB formation in ATM-deficient cells. To test this prediction, we used a previously described transgene (*Xmr-Spo11β*$_B$) that expresses the SPO11β isoform[18]. Indeed, there was substantial further elevation of SPO11-oligo complex levels (20.9 ± 1.5-fold over wild-type littermates, n=3) upon introduction of this transgene in an *Atm*-null background with intact endogenous *Spo11* (Fig. 3b). By contrast, the transgene resulted in only a modest increase in SPO11-oligo complexes in an ATM-proficient background (1.1 ± 0.05-fold, n=3) (Fig. 3b).

SPO11-oligo complexes from *Atm*-null testes were consistently shifted to a higher electrophoretic mobility compared to wild type or other mutants (Figs 1, 2b, 3). To examine the distribution of oligo lengths, labeled complexes were protease-digested and the resulting oligos were electrophoresed on a high-resolution gel (Fig. 4a). As previously shown[5],

SPO11-oligos from wild type have a bimodal length distribution with prominent subpopulations at apparent sizes of ~15–27 and ~31–35 nucleotides. *Atm*$^{-/-}$ mice showed a different pattern with or without the *Spo11* transgene: oligos in the shorter size range were less abundant relative to the ~31–35 nucleotide class, and longer oligos appeared, including an abundant class of ~40–70 nucleotides and a subpopulation that ranged to >300 nucleotides. *Spo11*$^{+/-}$ *Atm*$^{-/-}$ mice displayed an intermediate pattern, with more pronounced enrichment of the ~31–35 nucleotide class relative to both smaller and longer oligos. These results suggest that ATM influences an early step in nucleolytic processing of meiotic DSBs, as has been proposed in yeast[23]. In principle, altered oligo sizes could reflect changes in preferred positions of the endonucleolytic cleavage that releases the SPO11-oligo complex, effects on 3′→5′ exonucleolytic digestion of SPO11-oligos after they are formed, or occurrence of SPO11-induced DSBs at adjacent positions on the same DNA duplex (M. Neale, personal communication). Resection defects and adjacent DSBs (which conventional cytology would be unable to resolve) are both possible explanations for why SPO11-oligo complexes in *Atm*$^{-/-}$ spermatocytes show a greater increase than RAD51 focus numbers[14].

Our results reveal an essential but previously unsuspected function for ATM in controlling the number of SPO11-generated DSBs. We suggest that activation of ATM by DSBs triggers a negative feedback loop that leads to inhibition of further DSB formation (Fig. 4b) via phosphorylation of SPO11 or its accessory proteins, several of which are known to be phosphorylated in budding yeast (e.g., ref. 24) and are conserved in mammals[2]. ATM is activated in the vicinity of DSBs, as judged by SPO11- and ATM-dependent appearance of γH2AX (phosphorylated histone variant H2AX) on chromosomes at leptonema[12,13,25]. Thus, we envision that the negative feedback loop operates at least in part at a local level, perhaps discouraging additional DSBs from forming close to where a DSB has already formed. Such a mechanism could minimize instances where both sister chromatids are cut in the same region, and could also promote more even spacing of DSBs along chromosomes. These studies provide a new molecular framework for understanding the gonadal phenotypes of patients with ataxia telangiectasia[26], which is caused by ATM deficiency[27].

Methods Summary

Mouse mutant alleles and the *Spo11β* transgene were previously described[10,18,28–30]. Experimental animals were compared with controls from the same litter. Experiments conformed to regulatory standards and were approved by the MSKCC Institutional Animal Care and Use Committee. For measurement of SPO11-oligo complexes, both testes from each mouse were used per experiment, i.e., littermate comparisons were made on a per-testis basis (Supplementary Fig. 1). Testis extract preparation, immunoprecipitation, and western analysis were performed essentially as described[7]. Radiolabeled species were quantified with Fuji phosphor screens and ImageGuage software. The anti-mSPO11 monoclonal antibody was produced from hybridoma cell line 180 (M.P.T., unpublished). The size distribution of SPO11-oligos was determined essentially as described[5] after radiolabeling with [α-^{32}P] cordycepin. Benzonase treatment of SPO11-oligo complexes followed manufacturer's instructions (Novagen).

Methods

Testes were decapsulated, then lysed in 800 μl lysis buffer (1% Triton X-100, 400 mM NaCl, 25 mM HEPES-NaOH at pH 7.4, 5 mM EDTA). Lysates were centrifuged at 100,000 rpm (355,040 g) for 25 min in a TLA100.2 rotor. Supernatants were incubated with anti-mSPO11 antibody 180 (5 μg per pair of testes) at 4°C for 1 h, followed by addition of 30–40 μl protein-A–agarose beads (Roche) and incubation for another 3 h. Beads were washed three times with IP buffer (1% Triton X-100, 150 mM NaCl, 15 mM Tris-HCl at pH 8.0). Immunoprecipitates were eluted with Laemmli sample buffer and diluted 6- to 7-fold in IP buffer. Eluates were incubated with additional anti-mSPO11 antibody 180 at 4°C for 1 h, followed by addition of 30–40 μl protein-A–agarose beads and incubation at 4°C overnight. Beads were washed three times with IP buffer and twice with buffer NEB4 (New England BioLabs). SPO11-oligo complexes were radiolabeled at 37°C for 1 h using terminal deoxynucleotidyl transferase (Fermentas) and [α-^{32}P] dCTP. Beads were washed three times with IP buffer, boiled in Laemmli sample buffer and fractionated on 8% SDS–PAGE. Complexes were transferred to a PVDF membrane by semi-dry transfer (Bio-Rad). Radiolabeled species were detected and quantified with Fuji phosphor screens and ImageGuage software. For western analysis, membranes were probed with anti-mSPO11 antibody 180 (1:2,000 in PBS containing 0.1% Tween 20 and 5% non-fat dry milk), then horseradish-peroxidase-conjugated protein A (Abcam; 1:10,000 in PBS containing 0.1% Tween 20 and 5% non-fat dry milk), and detected using the ECL+ reagent (GE Healthcare). The size distribution of SPO11-oligos was determined by radiolabeling with [α-^{32}P] cordycepin then protease digestion followed by denaturing PAGE. Benzonase treatment of SPO11-oligo complexes was performed per manufacturer's instructions (Novagen).

Supplementary Material

Refer to Web version on PubMed Central for supplementary material.

Acknowledgments

We thank Matthew Neale for discussions, Rita Cha and Kim McKim for sharing data prior to publication, and Mona Hwang for assistance in monoclonal antibody development. This work was supported by NIH grants HD040916 and HD053855 (to M.J. and S.K.) and GM058673 (to S.K.). J.P. was supported in part by a Leukemia and Lymphoma Society Fellowship and F.C. by a Ruth L. Kirschstein NRSA (F32 HD51392). S.K. is an Investigator of the Howard Hughes Medical Institute.

References

1. Keeney, S. Recombination and Meiosis: Crossing-Over and Disjunction Vol. 2 Genome Dynamics and Stability. Lankenau, DH., editor. Springer-Verlag; 2007. p. 81-123.
2. Cole F, Keeney S, Jasin M. Evolutionary conservation of meiotic DSB proteins: more than just Spo11. Genes Dev. 2010; 24:1201–1207. [PubMed: 20551169]
3. Sasaki M, Lange J, Keeney S. Genome destabilization by homologous recombination in the germ line. Nat Rev Mol Cell Biol. 2010; 11:182–195. [PubMed: 20164840]
4. Hochwagen A, Amon A. Checking your breaks: surveillance mechanisms of meiotic recombination. Curr Biol. 2006; 16:R217–R228. [PubMed: 16546077]
5. Neale MJ, Pan J, Keeney S. Endonucleolytic processing of covalent protein-linked DNA double-strand breaks. Nature. 2005; 436:1053–1057. [PubMed: 16107854]

6. Pan J, et al. A hierarchical combination of factors shapes the genome-wide topography of yeast meiotic recombination initiation. Cell. 2011; 144:719–731. [PubMed: 21376234]
7. Daniel K, et al. Meiotic homologue alignment and its quality surveillance are controlled by mouse HORMAD1. Nat Cell Biol. 2011; 13:599–610. [PubMed: 21478856]
8. Barlow C, et al. Atm-deficient mice: a paradigm of ataxia telangiectasia. Cell. 1996; 86:159–171. [PubMed: 8689683]
9. Xu Y, et al. Targeted disruption of ATM leads to growth retardation, chromosomal fragmentation during meiosis, immune defects, and thymic lymphoma. Genes Dev. 1996; 10:2411–2422. [PubMed: 8843194]
10. Barlow C, et al. Atm deficiency results in severe meiotic disruption as early as leptonema of prophase I. Development. 1998; 125:4007–4017. [PubMed: 9735362]
11. Di Giacomo M, et al. Distinct DNA-damage-dependent and -independent responses drive the loss of oocytes in recombination-defective mouse mutants. Proc Natl Acad Sci U S A. 2005; 102:737–742. [PubMed: 15640358]
12. Barchi M, et al. Surveillance of different recombination defects in mouse spermatocytes yields distinct responses despite elimination at an identical developmental stage. Mol Cell Biol. 2005; 25:7203–7215. [PubMed: 16055729]
13. Bellani MA, Romanienko PJ, Cairatti DA, Camerini-Otero RD. SPO11 is required for sex-body formation, and Spo11 heterozygosity rescues the prophase arrest of Atm−/− spermatocytes. J Cell Sci. 2005; 118:3233–3245. [PubMed: 15998665]
14. Barchi M, et al. ATM promotes the obligate XY crossover and both crossover control and chromosome axis integrity on autosomes. PLoS Genet. 2008; 4:e1000076. [PubMed: 18497861]
15. Keeney S, et al. A mouse homolog of the Saccharomyces cerevisiae meiotic recombination DNA transesterase Spo11p. Genomics. 1999; 61:170–182. [PubMed: 10534402]
16. Shannon M, Richardson L, Christian A, Handel MA, Thelen MP. Differential gene expression of mammalian SPO11/TOP6A homologs during meiosis. FEBS Lett. 1999; 462:329–334. [PubMed: 10622720]
17. Bellani MA, Boateng KA, McLeod D, Camerini-Otero RD. The expression profile of the major mouse SPO11 isoforms indicates that SPO11beta introduces double strand breaks and suggests that SPO11alpha has an additional role in prophase in both spermatocytes and oocytes. Mol Cell Biol. 2010; 30:4391–4403. [PubMed: 20647542]
18. Kauppi L, et al. Distinct properties of the XY pseudoautosomal region crucial for male meiosis. Science. 2011; 331:916–920. [PubMed: 21330546]
19. Romanienko PJ, Camerini-Otero RD. Cloning, characterization, and localization of mouse and human SPO11. Genomics. 1999; 61:156–169. [PubMed: 10534401]
20. Romanienko PJ, Camerini-Otero RD. The mouse Spo11 gene is required for meiotic chromosome synapsis. Mol Cell. 2000; 6:975–987. [PubMed: 11106738]
21. Bellve AR, et al. Spermatogenic cells of the prepuberal mouse. Isolation and morphological characterization. J Cell Biol. 1977; 74:68–85. [PubMed: 874003]
22. Eaker S, Cobb J, Pyle A, Handel MA. Meiotic prophase abnormalities and metaphase cell death in MLH1-deficient mouse spermatocytes: insights into regulation of spermatogenic progress. Dev Biol. 2002; 249:85–95. [PubMed: 12217320]
23. Terasawa M, Ogawa T, Tsukamoto Y, Ogawa H. Sae2p phosphorylation is crucial for cooperation with Mre11p for resection of DNA double-strand break ends during meiotic recombination in Saccharomyces cerevisiae. Genes Genet Syst. 2008; 83:209–217. [PubMed: 18670132]
24. Sasanuma H, et al. Cdc7-dependent phosphorylation of Mer2 facilitates initiation of yeast meiotic recombination. Genes Dev. 2008; 22:398–410. [PubMed: 18245451]
25. Mahadevaiah SK, et al. Recombinational DNA double-strand breaks in mice precede synapsis. Nat Genet. 2001; 27:271–276. [PubMed: 11242108]
26. Sedgwick, RP.; Boder, E. Handbook of Clinical Neurology Vol. 16 (60) Hereditary Neuropathies and Spinocerebellar Atrophies. de Jong, JMBV., editor. Elsevier Science Publishers; 1991. p. 347-423.
27. Savitsky K, et al. A single ataxia telangiectasia gene with a product similar to PI-3 kinase. Science. 1995; 268:1749–1753. [PubMed: 7792600]

28. Edelmann W, et al. Meiotic pachytene arrest in MLH1-deficient mice. Cell. 1996; 85:1125–1134. [PubMed: 8674118]

29. Pittman DL, et al. Meiotic prophase arrest with failure of chromosome synapsis in mice deficient for Dmc1, a germline-specific RecA homolog. Mol Cell. 1998; 1:697–705. [PubMed: 9660953]

30. Baudat F, Manova K, Yuen JP, Jasin M, Keeney S. Chromosome synapsis defects and sexually dimorphic meiotic progression in mice lacking Spo11. Mol Cell. 2000; 6:989–998. [PubMed: 11106739]

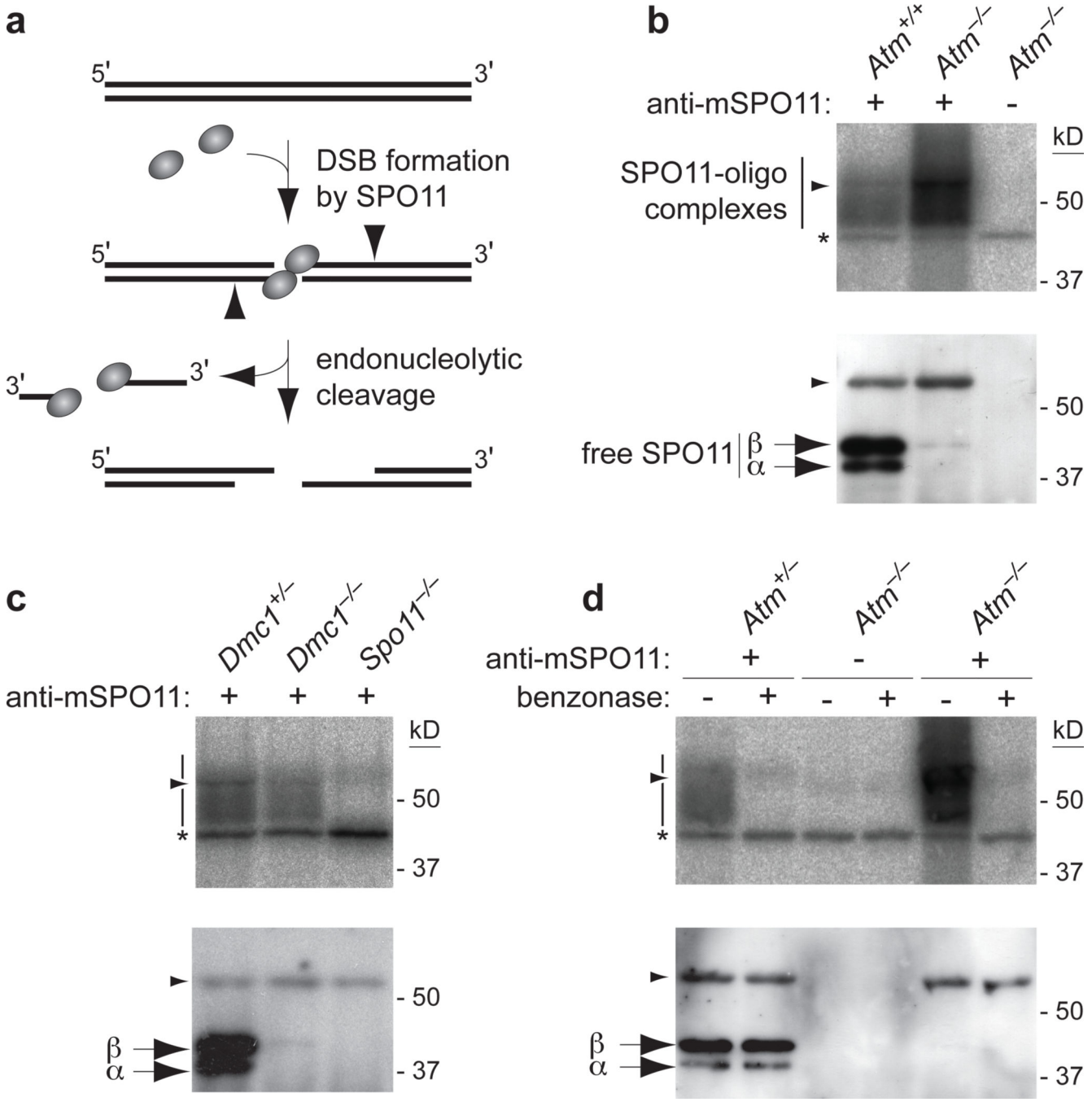

Figure 1. SPO11 activity and expression in the absence of ATM

a) SPO11 attacks the DNA phosphodiester backbone, forming a covalent intermediate with the 5′ strand termini of the DSB. Endonucleolytic cleavage removes SPO11 covalently attached to an oligonucleotide.

b, c) Steady-state levels of SPO11-oligo complexes are elevated in *Atm*$^{-/-}$ testes (b), but are decreased in *Dmc1*$^{-/-}$ testes (c). SPO11 immunoprecipitates from extracts of whole adult testes were treated with terminal transferase and [α-^{32}P] dCTP, resolved by SDS-PAGE, and transferred to a membrane. Representative experiments using littermates of the indicated

genotypes are shown. Upper panel, autoradiograph; lower panel, anti-SPO11 western detection. Bars, SPO11-specific signals; asterisk, non-specific terminal transferase labeling; arrowheads, migration position of immunoglobulin heavy chain.

d) Treatment of labeled SPO11 immunoprecipitates with benzonase does not detectably alter levels of free SPO11, but this sequence non-specific nuclease efficiently removes the 3′-end label (compare lanes ± benzonase), and was previously shown to completely remove DNA covalently bound to yeast Spo11 (ref. 1).

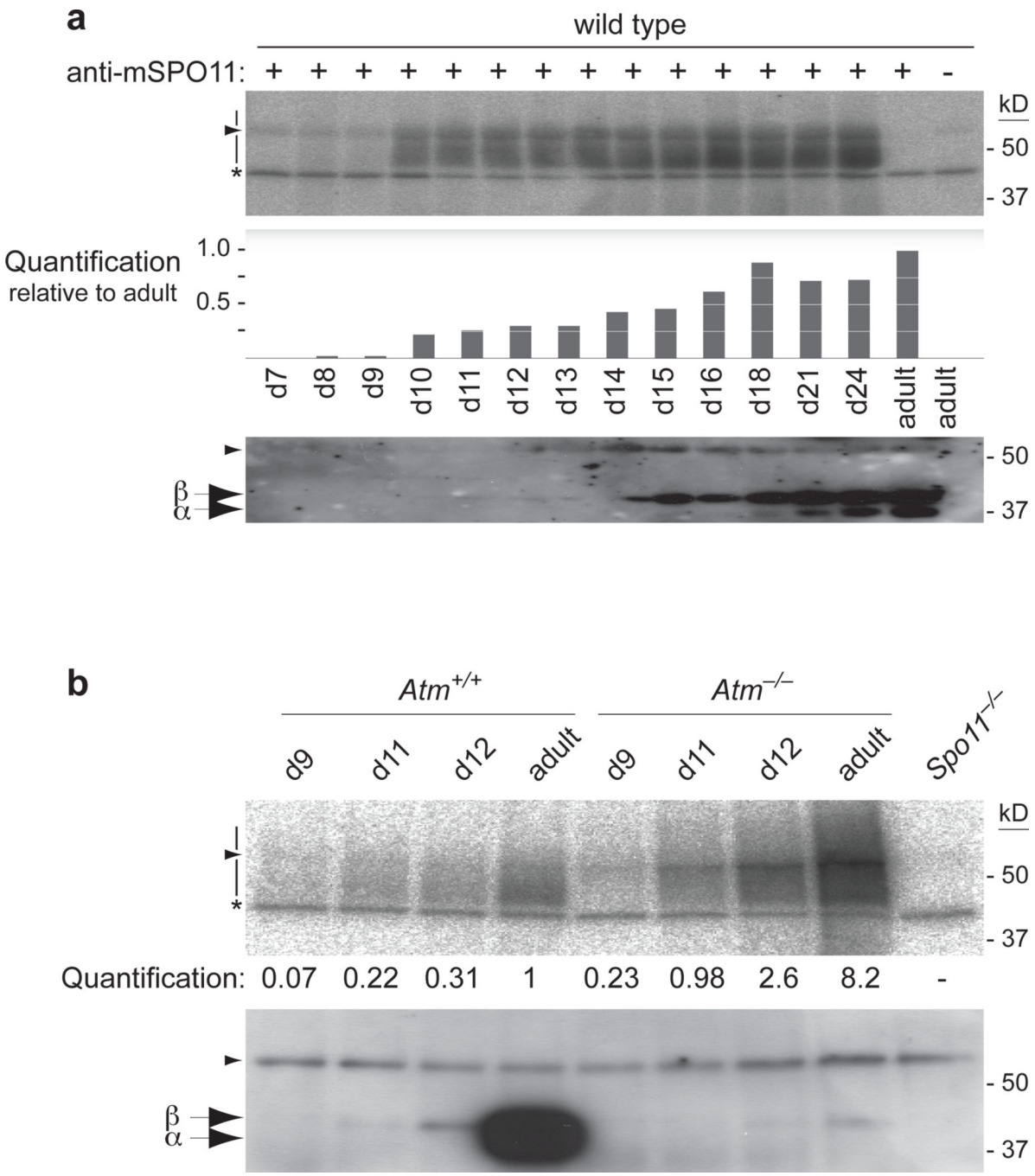

Figure 2. SPO11-oligo complexes from juvenile mice

a) SPO11-oligo complexes from testes of wild-type mice from post-natal days 7 to 24. Upper panel, autoradiograph; middle panel, quantification; lower panel, anti-SPO11 western detection.

b) SPO11-oligos are elevated in testes from juvenile *Atm*$^{-/-}$ mice. Upper panel, autoradiograph; lower panel, anti-SPO11 western detection.

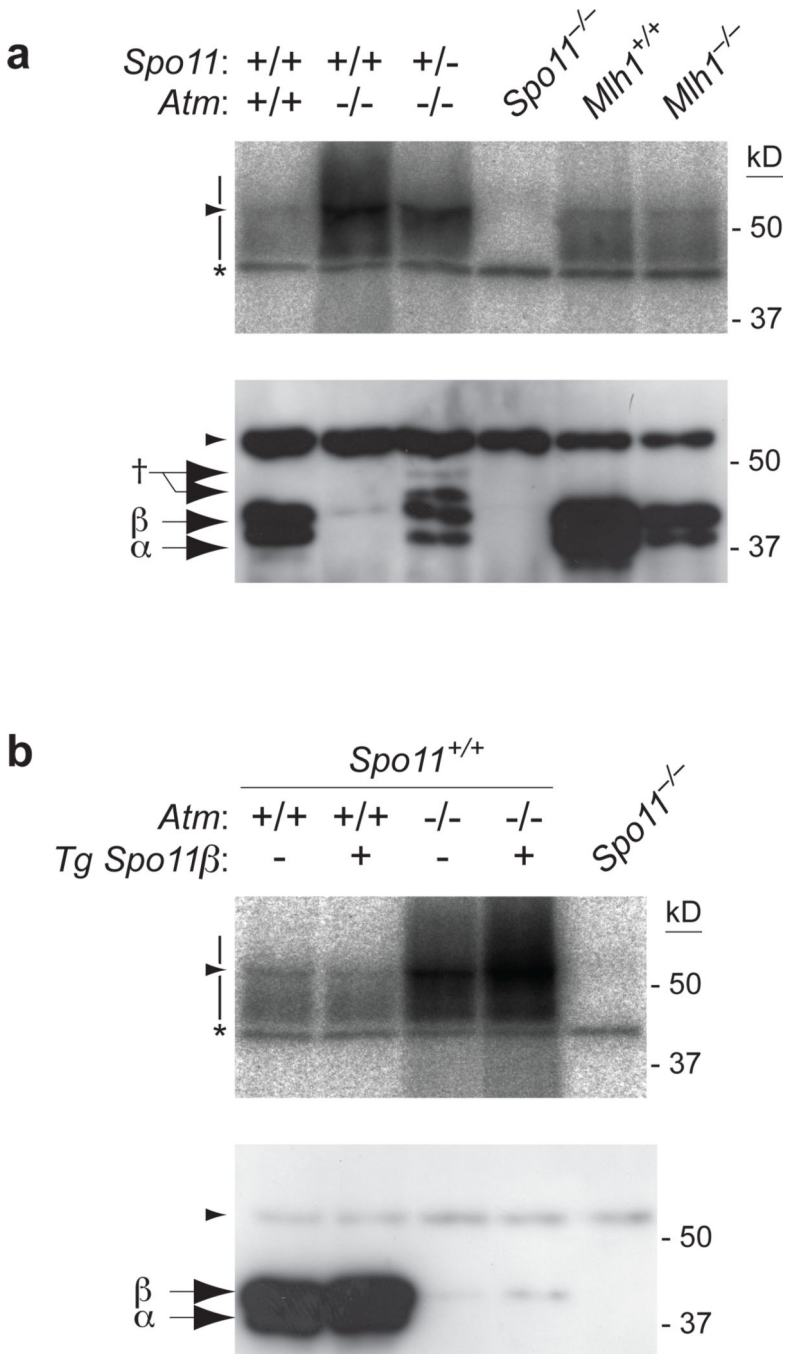

Figure 3. *Spo11* gene dosage modulates SPO11-oligo complex levels in *Atm*-deficient spermatocytes

a) SPO11-oligo complexes are reduced in *Spo11*$^{+/-}$ *Atm*$^{-/-}$ testes relative to *Atm*$^{-/-}$, but are more abundant than in wild type or in an *Mlh1*$^{-/-}$ mutant, which similarly arrests at metaphase. Consistent with further meiotic progression than *Atm*$^{-/-}$, both SPO11 isoforms (α and β) are expressed in *Spo11*$^{+/-}$ *Atm*$^{-/-}$ testes, although at reduced levels due to *Spo11* heterozygosity. Dagger, lower-mobility polypeptides likely originating from the *Spo11* knockout allele[18].

b) SPO11-oligo complexes are further elevated by SPO11β expression from the *Xmr-Spo11β*$_B$ transgene[18] in *Atm*$^{-/-}$ spermatocytes. Introducing this transgene into an otherwise wild-type background only modestly increased SPO11-oligo complex levels.

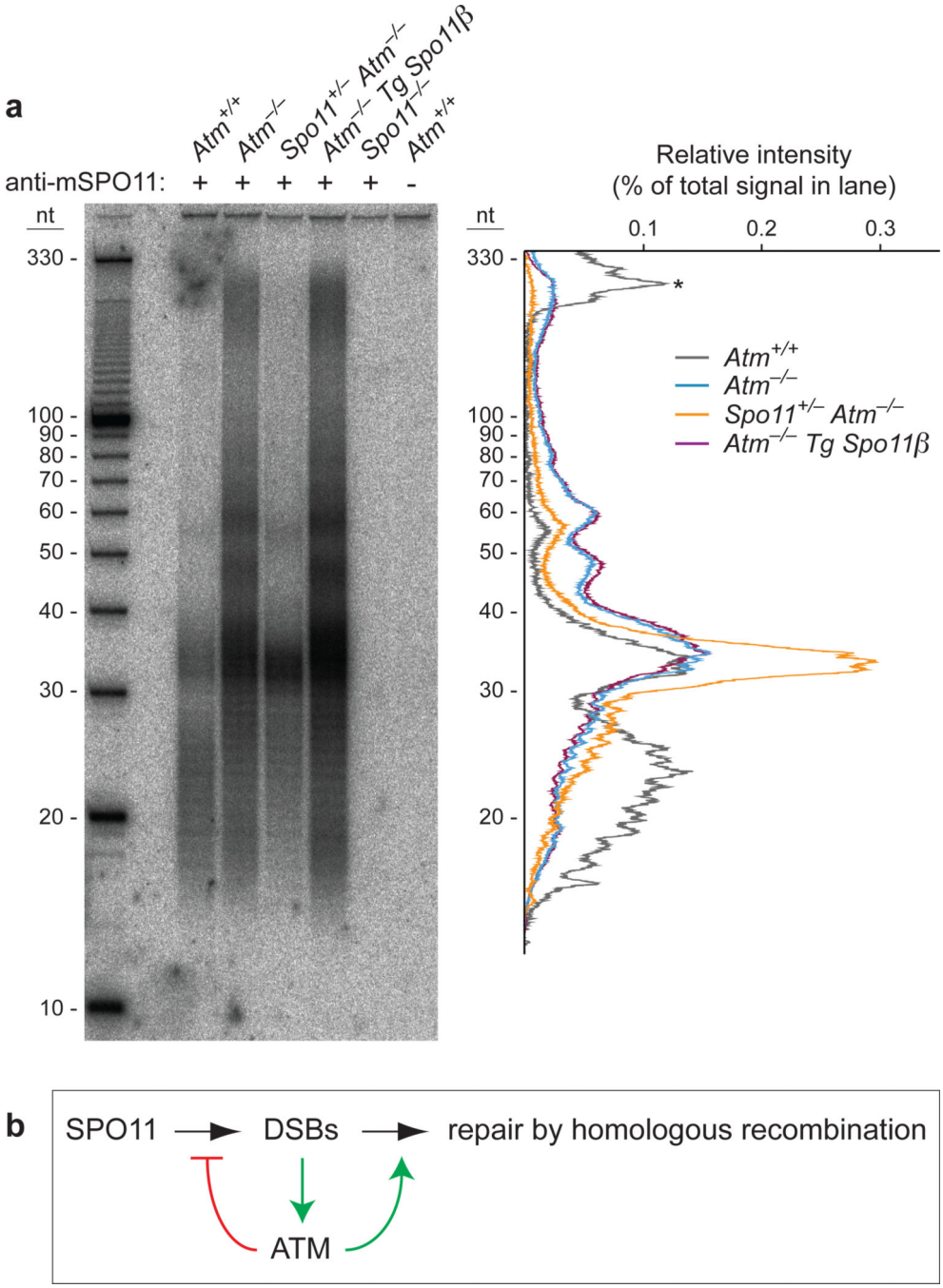

Figure 4. Roles of ATM in DSB formation and processing

a) SPO11-oligo length distribution is altered in *Atm*$^{-/-}$ spermatocytes. End-labeled SPO11-oligo complexes were treated with protease to digest the bound protein prior to electrophoresis on denaturing PAGE. Left panel, autoradiograph; right panel, background-subtracted lane traces normalized to total signal within each lane. Asterisk, autoradiograph background. Each lane contains SPO11-oligos from the equivalent of different numbers of mice in order to better compare sizes: *Atm*$^{+/+}$, 15 mice; *Atm*$^{-/-}$, 2 mice; *Spo11*$^{+/-}$ *Atm*$^{-/-}$, 4 mice; *Atm*$^{-/-}$ plus transgene, 2 mice; *Spo11*$^{-/-}$, 2 mice; mock, 15 wild-type mice.

b) Negative feedback loop by which ATM regulates meiotic DSB levels. DSBs generated by SPO11 activate the ATM kinase, inhibiting further DSB formation. ATM may also have roles in repair of DSBs by homologous recombination, for example, by promoting DSB end-resection.